Electronic Supplementary Information (ESI)

The Strong Jahn-Teller Distortion in Mn_3O_4-MnO Heterointerface for Enhanced Silver Catalyzed Formaldehyde Reforming into H_2

Xuehan Yu,[a] Kaicheng Qian,[a] Leilei Du,[a] Jiemei Zhang,[a] Nan Lu,[a] Ziqiang Miao,[a] Yuezhou Li,[a] Hisayoshi Kobayashi,[b] Xiaoqing Yan,[c] Renhong Li*[a]

[a] National Engineering Lab for Textile Fiber Materials and Processing Technology, School of Materials Science & Engineering, Zhejiang Sci-Tech University, Hangzhou, 310018, China.

[b] Emeritus Professor of Department of Chemistry and Materials Technology, Kyoto Institute of Technology, Matsugasaki, Sakyo-ku, Kyoto 606-8585, Japan.

[c] Department of Chemistry, College of Science, Zhejiang Sci-Tech University, Hangzhou 310018, China.

Corresponding Author

***lirenhong@zstu.edu.cn (Renhong Li)**

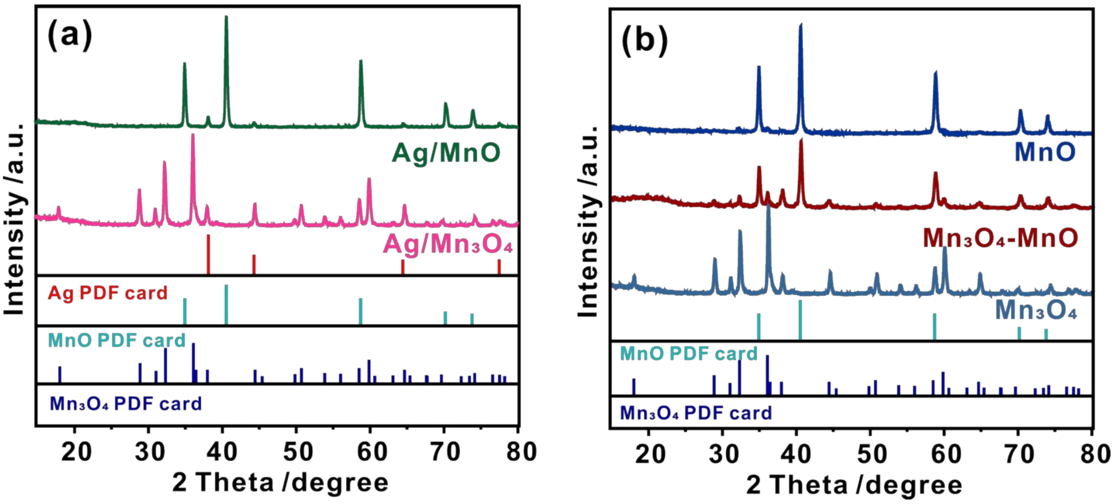

Figure S1. XRD patterns of (a) Ag/Mn_3O_4, Ag/MnO, (b) Mn_3O_4, Mn_3O_4-MnO, MnO.

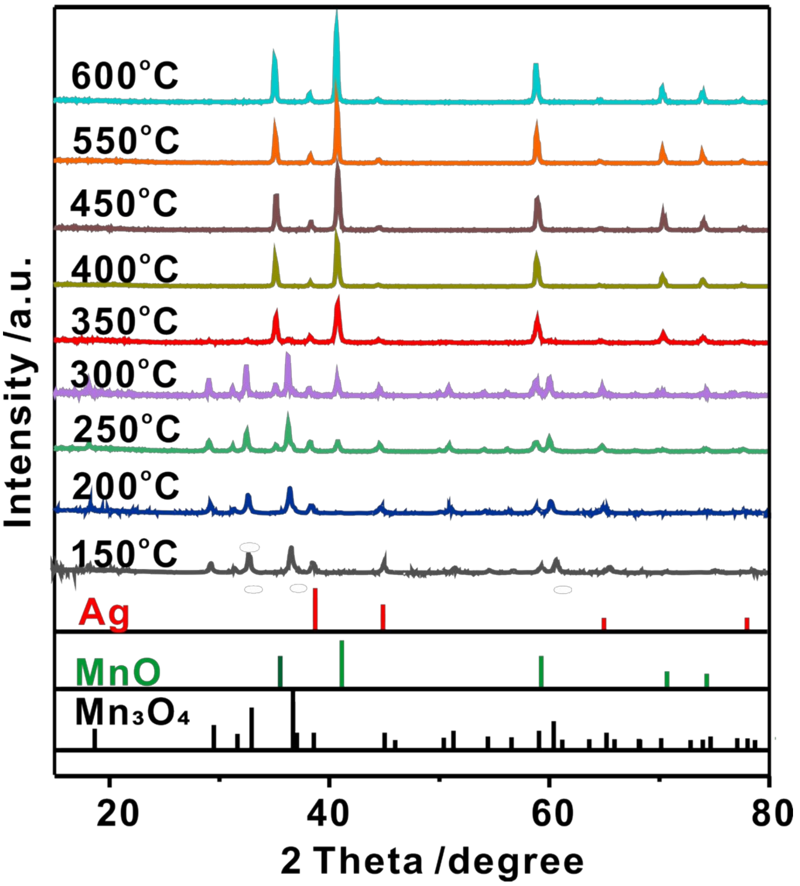

Figure S2. XRD images of different calcining temperature.

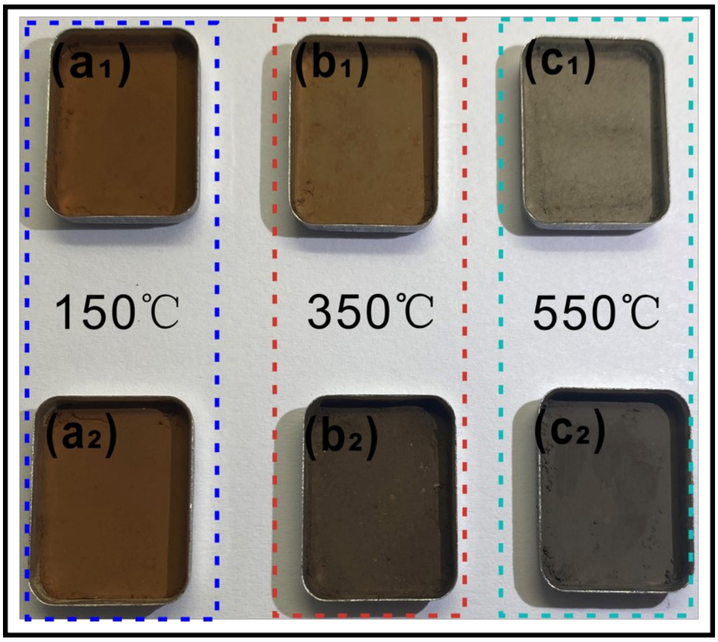

Figure S3. The color contrast before and after loading Ag at the calcination temperature of 150 °C, 350 °C, and 550 °C respectively.

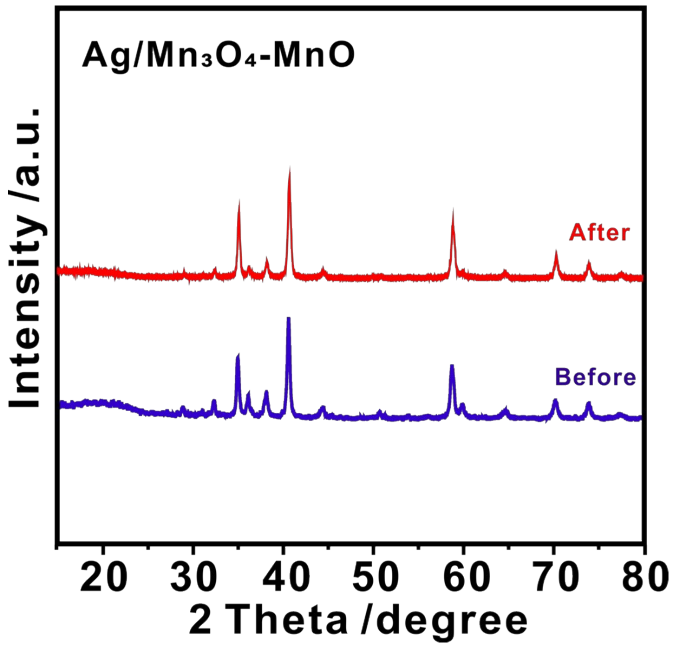

Figure S4. XRD patterns of Ag/Mn_3O_4−MnO before and after the catalytic reaction.

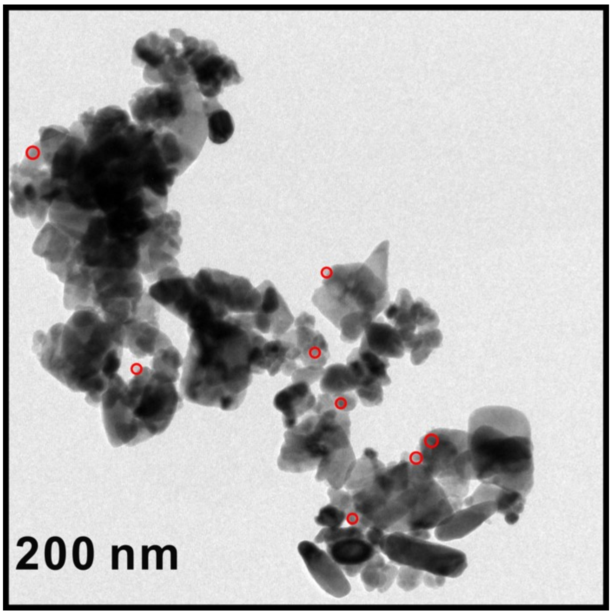

Figure S5. TEM image of Ag/Mn_3O_4–MnO.

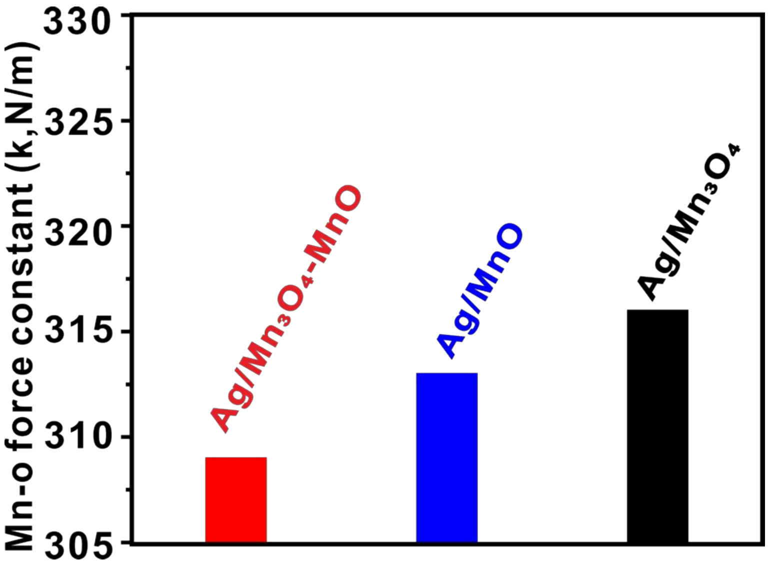

Figure S6. The corresponding Mn–O bond force constant of Ag/Mn_3O_4, Ag/Mn_3O_4–MnO, Ag/MnO.

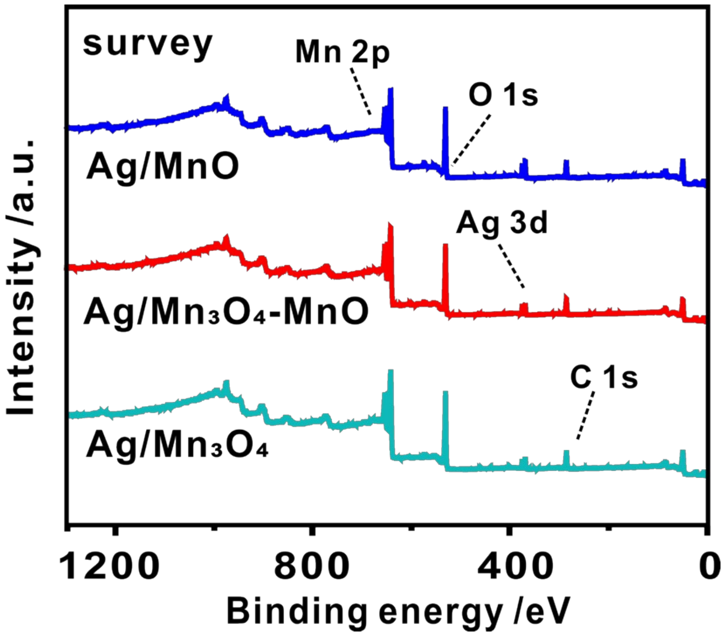

Figure S7. The full-survey-scan XPS spectrum of Ag/Mn_3O_4, Ag/Mn_3O_4−MnO, Ag/MnO.

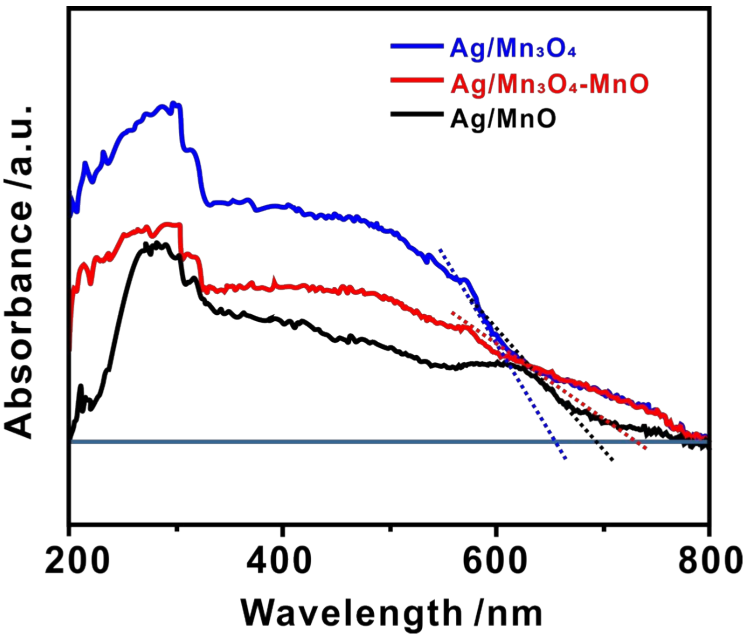

Figure S8. UV-visible absorption spectra of Ag/Mn_3O_4, Ag/Mn_3O_4-MnO, Ag/MnO.

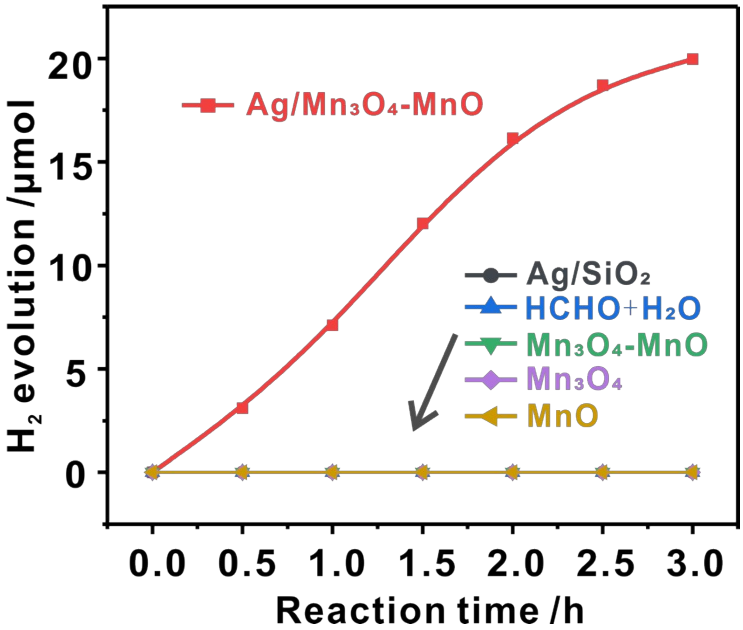

Figure S9. The catalytic hydrogen evolution performance of different component materials (Ag/Mn_3O_4-MnO, Ag/SiO_2, Mn_3O_4, Mn_3O_4-MnO, MnO) and HCHO+H_2O (T = 25 °C).

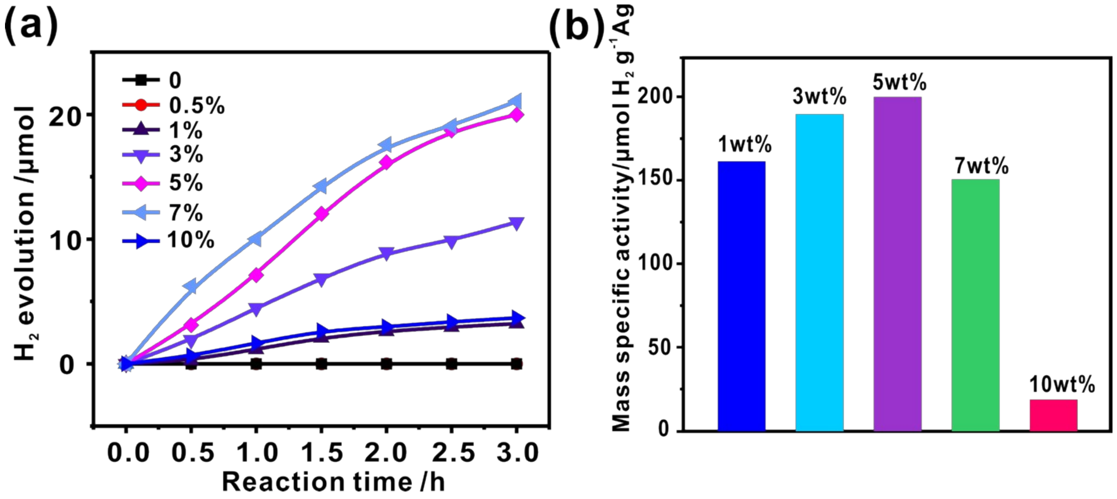

Figure S10. (a) The effect of different metal loading amount on the rate of H_2 evolution within 3 h reaction, (b) Comparison of mass specific activity of H_2 evolution rate based on silver metal within 3 h reaction, the catalytic reactions were carried out with 1 M HCHO at room temperature (25 °C) in $N_{2.}$

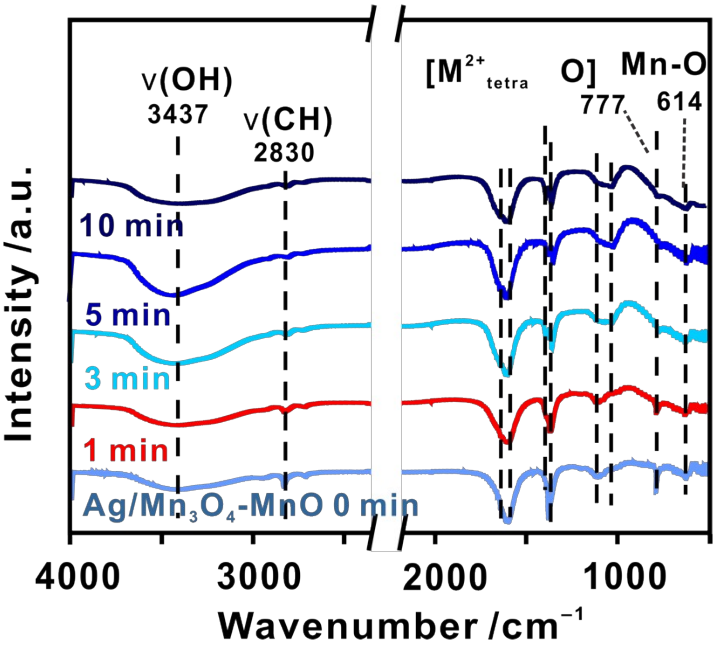

Figure S11. FT-IR spectra of fresh Ag/Mn_3O_4–MnO samples were collected different reaction times during HCHO solution dehydrogenation in the wavenumber range of 500-4000 cm^{-1}.

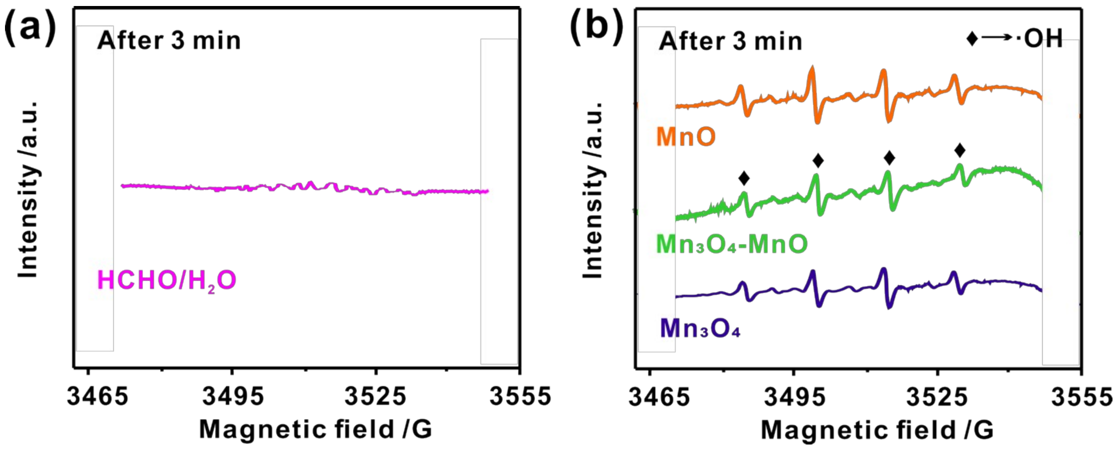

Figure S12. DMPO adducts recorded in the presence of (a) $HCHO/H_2O$, (b) Mn_3O_4, Mn_3O_4–MnO, MnO catalysts. All reactions were conducted in 1 M HCHO solution at 25 °C.

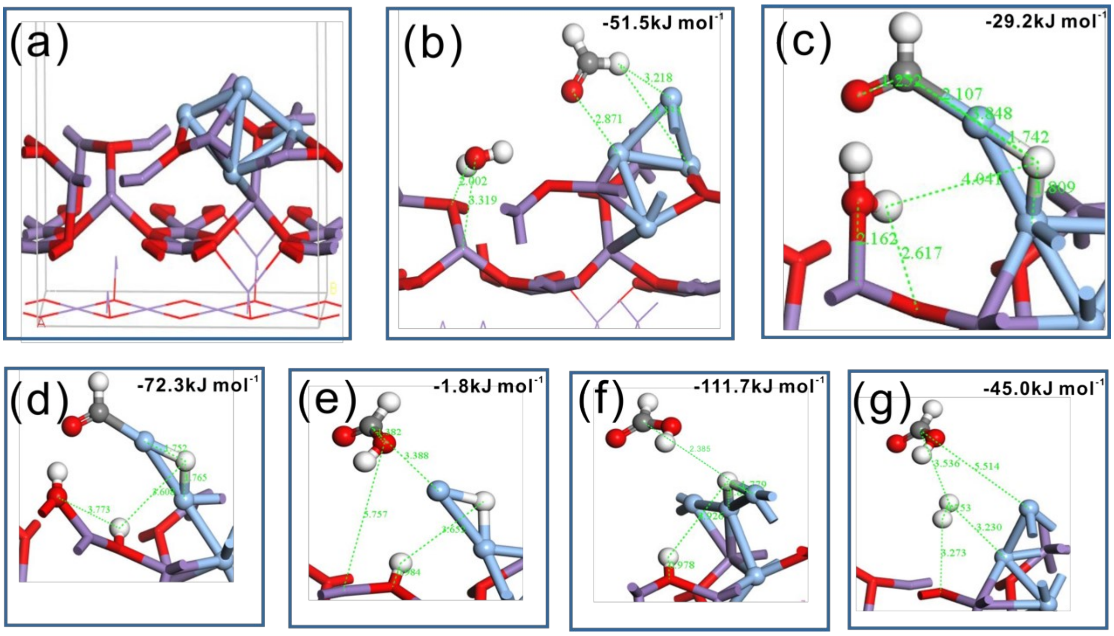

Figure S13. (a) $(Mn_8O_{10})_2Ag_4$ model, (b) $(Mn_8O_{10})_2Ag_4$-H_2O-H_2CO co-adsorption (conf#1), with an activation energy of −51.5 kJ mol^{-1}, (c) Co-adsorbed state of H, CHO, and H_2O (conf#3), the relative energy is −29.2 kJ mol^{-1}, (d) Co-adsorbed state of 2H, CHO, and OH (conf#5) (−72.3 kJ mol^{-1}), (e) Co-adsorbed state of 2H and HCOOH (conf#7)(−1.8 kJ mol^{-1}), (f) Co-adsorbed state of 2H and HCOOH (conf#8)(−111.7 kJ mol^{-1}). The H atom bonded to Ag atoms is rotated to the H−O side, (g) Final configuration of H_2 and HCOOH (conf#10) (−45.0 kJ mol^{-1}).

Table S1. Comparisons of the catalysts properties during HCHO reforming reaction into H_2.

Entry	Catalyst	[HCHO]/M ^{a}	T/^{o}C b	TOF/h^{-1}	t/h ^{c}	Additive ^{d}	Refs.
1	Cu NPs	0.5	18	1.67	3	NaOH	Ref.1
2	Pd NPs	0.5	25	47.6	1.67	NaOH	Ref.2
3	Ag NPs	0.5	25	62.6	0.83	NaOH	Ref.3
4	U/MnO_2	1.5	30	2.7	1	NaOH	Ref.4
5	Pd/TiO_2	0.6	25	71	0.5	NaOH	Ref.5
6	Ag NPs/SiO_2	1	25	0	3	—	This work
7	AgNPs/Mn_3O_4-MnO	1	25	22.2	3	—	
8	AgNPs/Mn_3O_4	1	25	0	3	—	
9	AgNPs/MnO	1	25	0	3	—	
10	Mn_3O_4	1	25	0	3	—	
11	MnO	1	25	0	3	—	
12	Mn_3O_4-MnO	1	25	0	3	—	

a concentrations of HCHO, b reaction temperature, c reaction time, d the additives used in the catalytic systems.

Notes and references

1. Y. Bi and G. Lu, *International J Hydrogen Energy*, 2008, **33**, 2225-2232.
2. H. Hu, Z. Jiao, J. Ye, G. Lu and Y. Bi, *Nano Energy*, 2014, **8**, 103-109.
3. Y. Bi, H. Hu, Q. Li and G. Lu, *J Hydrogen Energy*, 2010, **35**, 7177-7182.
4. L. Miao, Q. Nie, J. Wang, G. Zhang and P. Zhang, *Appl Catal B*, 2019, **248**, 466-476.
5. S. Li, H. Hu and Y. Bi, *J Mater Chem A*, 2016, **4**, 796-800.